36th International Electric Vehicle Symposium and Exhibition (EVS36)
Sacramento, California, June 11-14, 2023

Novel Sensing Techniques for Lithium-ion Battery Modeling and States Estimation

Xia Zeng[1,#], Pavlo Ivanchenko[1], Theodoros Kalogiannis[1], Joeri Van Mierlo[1], Maitane Berecibar[1]
[1]*MOBI Research Center & Department ETEC, Vrije Universiteit Brussel, Pleinlaan 2, 1050 Brussels, Belgium.*
[#]*Corresponding author (xia.zeng@vub.be)*

Executive Summary

The increasing dependence on batteries calls for the accurate monitoring of battery functional status to increase their quality, reliability, and life. This has led to a variety of ingenious approaches developed over the years, among which the utilization of novel sensors is attracting increasing attention. Rather than summarizing all relevant previous work in novel sensing-based battery states monitoring, this paper selects noteworthy work that may suggest crucial future trends of applying novel sensing techniques to enhance the physics-guided functionalities in the battery management system. With ultrasonic sensors as an example, their working principles and general application in non-destructive detection are introduced. The ultrasonic evaluation for a commercial lithium-ion pouch cell is performed. The experiment results show that features from ultrasonic measurements could be potential parameters to determine the battery state-of-charge. The discussion presented herein is expected to induce a more fluent exchange of ideas and more intense interest in this emerging field. Future studies will present more on novel sensors and their benefits, drawbacks, possibilities and applications in battery domain.

Keywords: Batteries, Ultrasonic sensors, In operando, State estimation, Diagnostics and prognostics.

1 Introduction

The need to decarbonize the transportation sectors has led to the rapid electrification of transportation and the growth of large-scale energy storage systems, which further promoted the gradual dominance of lithium-ion batteries (LIBs) in the market due to their high energy density, low self-discharge, and long cycling life [1, 2]. This trend has, on the one hand, led to the developing of various types of batteries, such as solid-state batteries [3]; on the other hand, increased the public anxieties regarding fast charging [4], electric vehicle range [5], and safety concerns [6]. These challenges pose significant milestones to the efficient functioning of battery management systems (BMS), which typically rely on conventional measurements such as current, voltage, and temperature to perform real-time state monitoring, charge/discharge control, and thermal management [7, 8]. To address these challenges, BMS needs to be promoted with more advanced functionalities, including but not limited to online monitoring and optimization of battery performance under harsh conditions, predicting the remaining useful life (RUL) of batteries using only early-life datasets [9], and detecting and/or preventing battery failures using non-destructive techniques [10].

Though extensive research has been carried out to develop the above milestones, there are still several challenges that need to be addressed. The online monitoring of internal states and degradation is difficult during battery regular operation, given the limited number of measured quantities and the effect of measurement noise. Most of the estimation schemes rely on measurement accuracy and may overlook

instrumentation malfunctions. Moreover, the estimation accuracy of battery states is highly influenced by aging mechanisms, which arise from a complex interplay of physical and chemical phenomena affected by environmental conditions, usage patterns, and operational history [11, 12, 13, 14]. A large number of degradation mechanisms and their inter-dependencies pose significant challenges for modeling and detecting degradation in Li-ion cells.

A push to develop new monitoring techniques for LIBs has led to spectacular advances across novel sensing techniques, with which the battery will no longer be simply a black box. The primary idea is to inject inside and/or attach the battery surface with various smart sensing technologies and functionalities, such that one can passively monitor the effects of temperature, pressure, and strain, with more physical information transmitting in and out of the cells [15]. Hereby, we present an overview of the status determination with novel sensing techniques. The working principles of ultrasonic sensors and a case study with in operando ultrasonic signal evaluation are also described.

2 Novel sensing techniques for lithium-ion battery application

A sensor is a device that detects and converts non-electrical effects into electrical signals, typically requiring one or several transformation steps to produce the desired electric output signal [16]. In the field of battery management, sensors are widely used to monitor various parameters, such as voltage, current, and temperature. This section focuses on highlighting different types of sensors that can provide physical insights into the battery.

Based on their measurements or stimuli, the commonly used sensors in the battery application domain could be grouped as a) electric sensors with voltage and current measurement, b) thermal sensors with temperature, flux, and specific heat measurement, c) mechanical sensors with pressure, strain, and stress measurement, and d) acoustic/ultrasonic sensors with wave amplitude, phase, spectrum measurement [16]. Measurements from the first two groups enable a large proportion of the battery management tasks in the presented literature and engineering practice [17, 18]. However, emerging sensor technologies, such as those that measure force or pressure [19], cell internal strain [20], and time of flight (ToF) [21, 22, 23], show great promise in improving battery safety [24], lifetime, and sustainability [25].

Moreover, most of the aforementioned sensors rely on the use outside rather than inside the battery cells, limiting the knowledge to macroscopic properties and overlooking internal chemical/physical parameters of prime importance for monitoring battery lifetime. Throughout the entire life cycle of a LIB, complex electrochemical, mechanical, and thermal processes occur dynamically within the cell, regardless of its operational status [24]. During the charging process illustrated in Fig.1, for instance, lithium-ions are extracted from the cathode, traverse the separator, and inserted in the anode. This dynamic process produces reversible and irreversible thermal generation and volumetric changes in the cell. Under normal operating conditions, the battery surface and core often exhibit significant temperature differences [26, 27, 28]. The degree of expansions at cell level mainly depends on the used electrode materials and battery structure (cylindrical, pouch or prismatic). Naturally, these volumetric changes will result in a counter force against any applied external pressure on the cell surface [19]. Several studies have shown that the anode contributes more significantly to the overall cell expansion [29, 30]. Therefore, in addition to conventional attached sensors, embedded/implantable sensors are increasingly employed to gain deeper insights into the macroscopic properties and internal chemical/physical parameters [31].

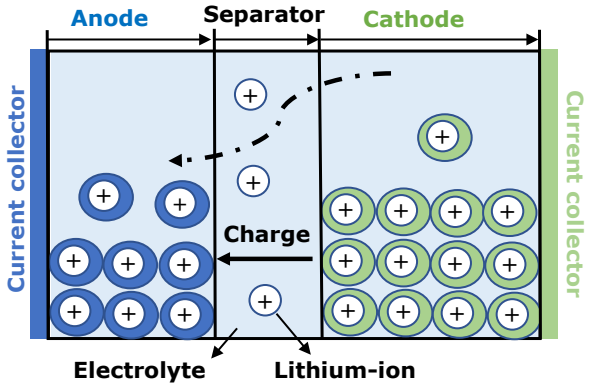

Figure 1: Working principle of a LIB during charge, where the dot-dashed line presents the movement of lithium-ions.

With implantable sensors attracting increased interest, optical sensing is predominant [32, 33, 34]. The lightweight, flexible, and low-cost optical fibers make it possible for them to be embedded into individual cells without significant additional size and weight [35]. Furthermore, the high sensitivity and multiplexing capability to measure a wide range of parameters of interest for fiber optic sensing (FOS) allows them to detect strain, acoustic emission, and chemical species formation inside the battery, which could sever as strong indications of battery states [35, 25]. However, there are still several challenges to the practical implementation of FOS in battery applications. Concerns about cost pose the most substantial roadblock to enhanced monitoring, especially cell-level monitoring. A few concerns have also arisen about the insertion safety of optical fibers into batteries and the durability of the materials both on the fiber side and the battery electrode [34, 35].

3 Battery monitoring with ultrasonic sensors

As discussed in Section 2, many efforts are being made to understand and monitor the battery with novel sensing techniques. Based on different working principles, each sensor can track various changes inside the battery and thus different parameters could be extracted to describe a battery state. However, for the sake of brevity, this section will only focus on the ultrasonic sensors.

3.1 Ultrasonic sensors

In analogy to visible and ultraviolet light, the terms ”sound” and ”ultrasound” are used to describe the propagation of a mechanical perturbation in different frequency ranges. Compared to acoustic sensors, ultrasonic sensors operate at higher frequencies and can detect sound waves beyond the audible range [36]. Due to their high sensitivity, versatility, and cost-effectiveness, both sensors have been widely used in non-destructive detection (NDT) and/or structure health management (SHM) [36, 37]. The schemes available for SHM can be broadly classified as active or passive depending on whether or not they involve the use of actuators, respectively. Guided-wave (GWs) testing has emerged as a very prominent option among active schemes. It can offer an effective method to estimate the location, severity, and type of damage, and it is a well-established practice in the NDT industry. There, GWs are excited and received in a structure using handheld transducers for scheduled maintenance. In ultrasonic testing, GWs with high-frequency sound energy can propagate as elastic waves through a material [36]. The measurements could then be used to detect defects such as corrosion or cracks that may not be visible from the outside. Thus, ultrasonic GWs are widely used for flaw detection/evaluation, dimensional measurements, material characterization, and more [38].

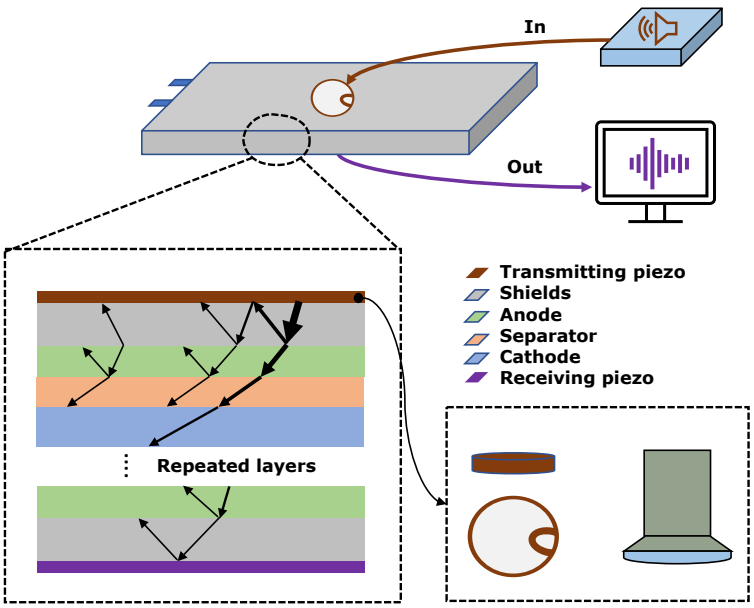

Figure 2: Schematic illustrations of ultrasonic testing with a pouch battery. Top: the experimental set-ups, including the signal generation and acquisition system and a pouch cell with transmitting and receiving piezos attached. Bottom left: the sound (represented by arrows) going through different layers of the cell, with some reflected and some transmitted. Bottom right: piezos of slice shape [Left] and probe transducers [Right].

The critical components of ultrasonic GWs include the transducers, relevant theory, signal processing methodology, the arrangement of the transducer network to scan the structure, and the overall SHM architecture (i.e., issues related to supporting electronics, robustness, and packaging) [39]. The most commonly used transducers are angled piezoelectric transducers, comb transducers, and electromagnetic acoustic transducers. The widely used piezoelectric transducers for SHM are embedded or surface-bonded piezoelectric wafer transducers (referred to as "piezos" hereafter). Piezos are inexpensive and available in very fine thicknesses, making them unobtrusive and conducive to integration into structures [39, 40]. The ultrasonic sensors with piezoelectric films are normally used to study the evolution of the acoustic waves transmitted through the battery [41, 42, 21, 22, 23]. With a pouch LIB as an example, Fig.2 presents a pitch-catch inspection configuration. The whole system includes several functional units, such as the pulser/receiver, transducers, and display devices. Depending on the application, different shapes and placements of transmitter and receiver are possible.

The pulser/receiver is an electronic device that can produce high-voltage electrical pulses. When driven by the pulser, the transducer generates high-frequency ultrasonic energy, which is introduced and propagated through the battery in the form of waves. As the initial pulse passes through each interface, some fraction of the wave is transmitted and some is reflected, depending on the degree of mismatch in the sound speed c between adjacent layers and whether c increases or decreases from one layer to the next. Additionally, the wave is attenuated (i.e., loses energy) as it passes through the bulk region of each layer. As each interface is an opportunity for the pulse to split, the acoustic behavior of the cell quickly becomes complicated. To be more specifically, each new wave interacts not only with interfaces (creating even more waves) but also with each other. Consequently, with the multi-layer structure for LIBs, the sound waves become increasingly dampened due to dissipation and the increasing number of encountered interfaces. The result is an "echo chamber" effect for reflected the waves. With all said, the received signal is a fusion datasets and hard to distinguish the exact echo for each layer.

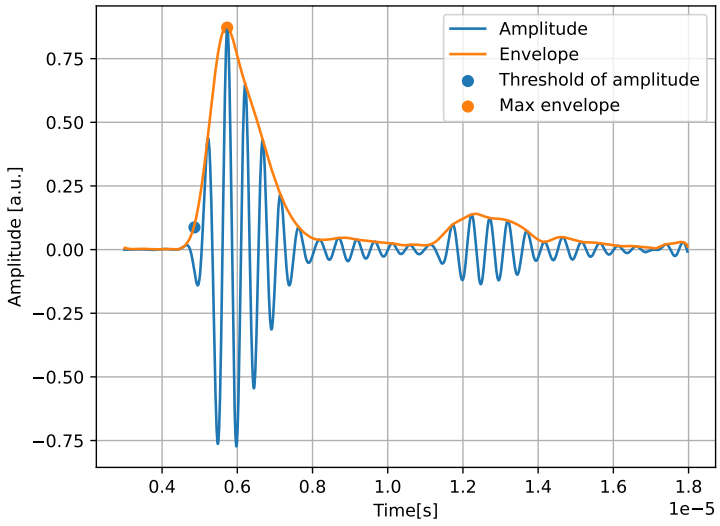

Figure 3: Example of transmitted signal in the time domain, including the envelope, maximum envelope, and 10% threshold of the absolute amplitude.

After crossing all the layers of the battery, the reflected wave signal is transformed into an electrical signal by the transducer. Depending on propagation mode, the propagation through the battery cell [22] or along its surface [43] can be measured [44]. With the received signals, various characteristics and information can be inferred and employed to potentially decide if damage has developed in the structure. Before extracting the features, pre-processing or data cleansing may be needed to clean the signals, since any sensor, in general, is susceptible to noise from a variety of sources [39]. This is particularly needed if the feature extraction mechanism is not robust to noise. Later, as shown in Fig.3, different features of interest could be extracted, which typically include the ToF, amplitude, and envelope in the time domain and power spectral density (PSD) in frequency domain [45]. The ToF is normally defined as the time difference between the sending and reception of the signal. Furthermore, the ToF allows the calculation of propagation speed and Young's modulus base on Equations 1 and 2, respectively, where c is the mean sound velocity, d is the cell thickness, E_{eff} is the effective Young's modulus, and ρ is the overall density of the battery. The amplitude of the transmitted signal can also be taken as a measure of the attenuation of the sound wave when passing through the medium [44].

$$c = \frac{d}{ToF} \tag{1}$$

$$c = \sqrt{\frac{E_{eff}}{\rho}} \tag{2}$$

With all the collected damage-sensitive features, a pattern recognition technique is required to classify the damage and estimate its severity. It's important to note that GWs SHM always involves the use of some threshold value to determine whether the damage is present in the structure or not. The choice of the threshold is usually application-dependent and typically relies on some false-positive probability estimation [39]. In the LIB application, patterns in different features (i.e. density, Young's modulus, the porosity of the electrodes) could be detected and further used to describe the battery state [46, 45]. The absolute energy signal strength and the PSD of the signal transmitted are considered to monitor the reversible change that occurs during the charge/discharge process. Variations noted can be correlated to the battery SoC [21, 46].

3.2 Case study: in operando ultrasonic signal evaluation

To see how ultrasonic waves could vary while a LIB is operating, this section will present a case study with one cell from KoKam (SLPB065070180, Kokam Co., Ltd.). The cell consists of a graphite anode and a nickel-rich NCM cathode. The battery cells have an active area dimension (excluding sealing and tabs) of 67 mm×165 mm (width×height). The thickness of the battery cell is 6.5 mm ±0.05 mm at SoC 30%. More specifications of this cell are summarized in Table 1.

Table 1: KoKam cell specifications

Characteristic	**Value**	**Units**
Cathode Composition	NCM	—
Nominal voltage	3.7	V
Maximum charge voltage	4.2	V
Minimum discharge voltage	2.7	V
Nominal capacity	12	Ah
Maximum charge current	12	A
Maximum discharge current	24	A

3.2.1 Experimental set-ups

Following the illustrations in Fig.2, the ultrasonic experiments are prepared with four essential components: 1) a battery sandwiched with ultrasonic transducers, 2) a PCUS pro-Single ultrasonic frontend (Fraunhofer Institute for Ceramic Technologies and Systems IKTS), which enables manual or automated inspections with a single conventional probe (single or dual elements), 3) a Biologic potentiostat (VMP3, VSP) with a booster to charge and discharge the cell, and 4) a laptop with another printed circuit board to control the PCUS and record the receiving signals.

The cell was sandwiched between two ultrasonic sheets, as illustrated in Fig.4. The 2 mm damping layers and the ultrasonic PZT discs, with 1 mm thick and 10 mm diameter, have been glued onto both sides of the battery. The ultrasonic transducers have a center frequency of 2 MHz. The signal evaluation was performed through the use of the PCUS electronics and Python scripts. The frequency, amplitude, and signal shape of the transmitted signal were set within the Python scripts. The transmitted ultrasonic waves were measured in the receiver and electronically amplified.

After setting up all the necessary equipment and placing the battery in a 25 °C thermal chamber, a rectangular pulse with 200 V and a length of 500 ns was continuously sent from the PCUS. As shown in Fig.2, the excited ultrasonic signal passed through the different layers inside the battery and the received waves was recorded by the PCUS analog-digital converter at a sampling rate of 100 MHz. Simultaneously, the battery started a constant current constant voltage (CCCV) charging and CC discharging. The current applied during CC charge and discharge was $C/2$ (6 A), and the cut-off criterion in the CV step during charge was a current of 0.05A at 4.2 V. After reaching the charging cutoff criterion, a 0.5 h rest period was included. The discharge stopped at the minimum voltage of 2.7 V and continued with a 0.5 h rest.

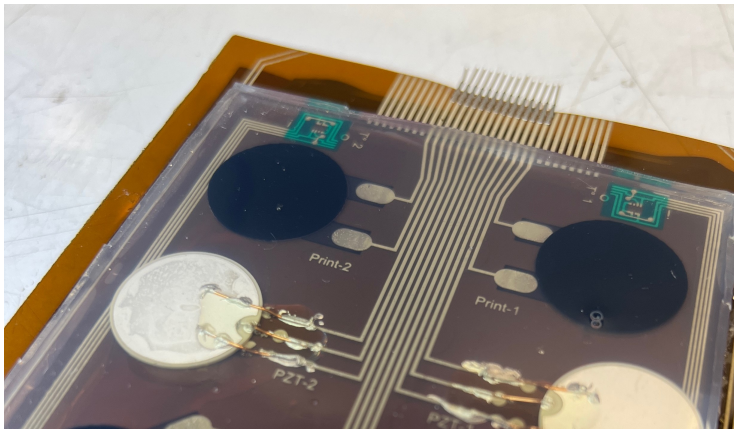

Figure 4: Details of the manufactured ultrasonic sensor system within a battery.

3.2.2 Results and discussion

After collecting and pre-processing data, various features were evaluated from the ultrasonic data. The sample waves collected from aforementioned tests are depicted in Fig.5. In this cell, as SoC drops during discharge, the first measured waves (from $0.4e{-}5$ to $0.8e{-}5$ seconds) undergo a significant change. The height and width of the amplitude decrease as the battery discharges. Additionally, the second set of waves (from $1.1e{-}5$ to $1.6e{-}5$ seconds) was also observed, which did not change significantly compared to the first waves. These behaviors become even more noticeable when examining the envelope in Fig.5. The maximum envelope decreases from 0.911 a.u. to 0.706 a.u. as the SoC drops from 0.8 to 0.2.

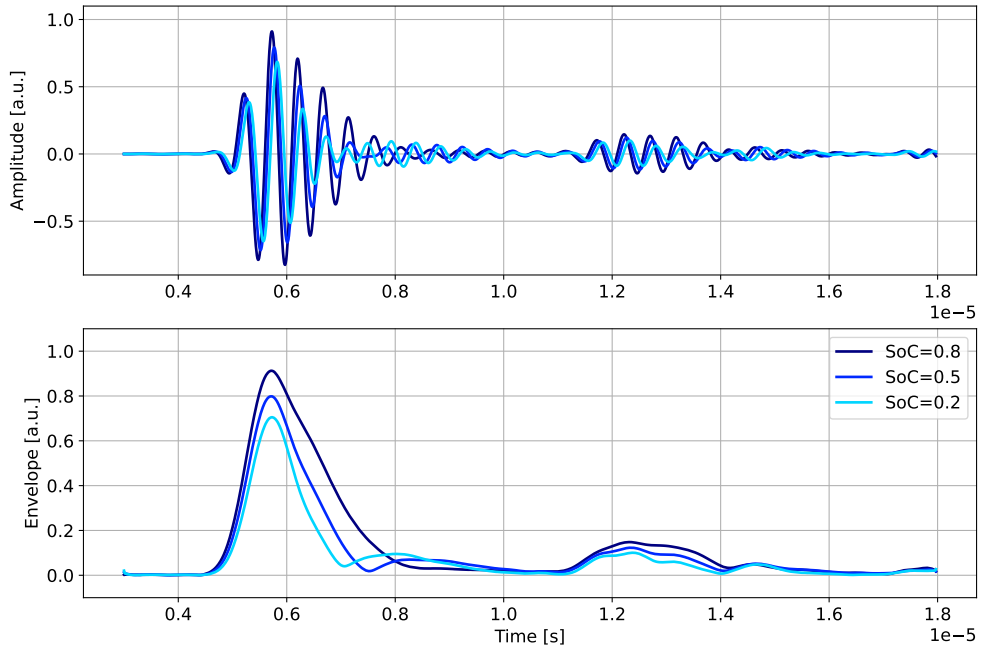

Figure 5: Amplitude [Upper] and envelope [Lower] at three different SoCs during $C/2$ discharge.

To further evaluate the ToF based on the amplitude, a thresholding method was utilized. The ToF was determined as the first data point of the entry that exceeded the threshold. The optimum threshold value is often estimated empirically. It can be chosen relative to the maximum of the measured signal, e.g. 5%. Ideally, the maximum of the measured signal lies within one of the transmitted acoustic wave packages. Otherwise more elaborate threshold value picking criteria may be required. Another option is to choose the threshold based on the noise since it should lie above the noise level to avoid false positives [47]. Hereby, the threshold was set at 10% of the absolute maximum amplitude, chosen as a suitable compromise between detecting the signal as early as possible and staying well above the noise level [45]. To improve the ToF resolution beyond the 10 ns limit imposed by the 100 MHz sampling rate of the A/D

converter, the signal was linearly interpolated between the first data point exceeding the threshold and the previous data point.

With the battery being charged and discharge, the maximum amplitude varies, as shown in Fig. 6. During CC charging, the maximum amplitude increases, and this increase continues during CV charging and rest periods. The maximum amplitude then decreases during discharge, as previously observed in Fig.5. Once the discharge is finished, a relatively small rise is also observed in the maximum amplitude, similar to the voltage recovery.

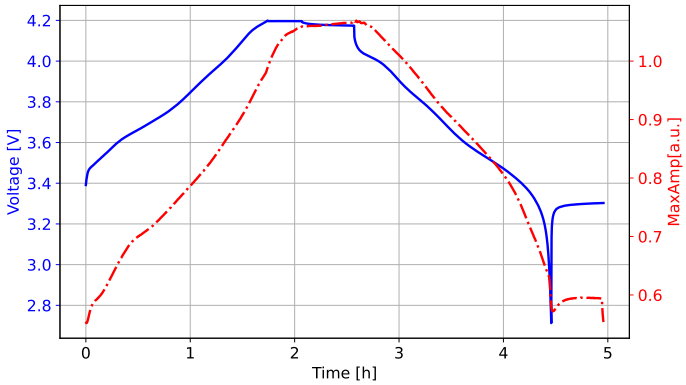

Figure 6: Voltage [Solid line] and maximum amplitude [Dot-dashed line] during $C/2$ charge and discharge.

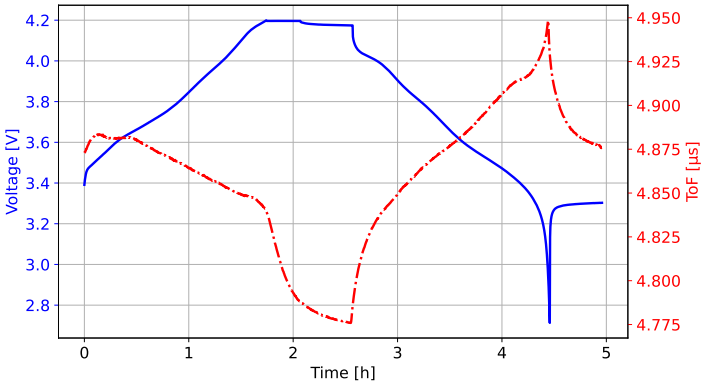

Figure 7: Voltage [Solid line] and ToF [Dot-dashed line] during $C/2$ charge and discharge.

Unlike the maximum amplitude, the ToF decreases with charging the battery, while increases with discharging it. Initially, this is counterintuitive as the cell is getting thicker during charging and thus the signals would need to traverse a greater distance. If the assumption on constant sound velocity holds, based on Equation 1, the ToF supposes to increase together with cell thickness during charge. However, with a measurement of cell thickness and based on Equation 2, recent study [45] has shown that, while battery is operating, the sound velocity changes, which is dependent on the change in stiffness of the electrodes inside the cell. To be more specific, the graphite in lithiated state is much harder/stiffer, thus causing higher effective Young's modulus, than graphite in the unlithiated state. Harder/stiffer materials transfer sound waves faster. Therefore the ToF of the charged cell is smaller. A plateau in the ToF is also observed when the battery started CV charging at 4.2 V. By comparing the differential ToF ($dToF/dV$) and differential voltage (dQ/dV) analysis in [45], such a plateau might potentially be associated with the phase transition of the NCM battery. More investigations into the estimation of SoC from ultrasonic data and the causes of the plateau will be given in our future studies.

4 Conclusions

Effective battery monitoring is crucial for ensuring reliable and safe operation of battery-powered devices. However, traditional sensors often prove inadequate for measuring several battery states, thus necessitating the development of novel sensing techniques. In this paper, a comprehensive overview of

the use of novel sensors in the battery domain is presented, together with discussions on their advantages and limitations. Then focusing on ultrasonic sensors, their working principles and representative examples of their application in NDT are described.

A case study using a commercial pouch battery is performed to demonstrate the potential of ultrasonic sensors for battery monitoring. The experimental results reveal that ultrasonic features, such as maximum amplitude and ToF, undergo significant changes during battery operation. These features hold promise for determining battery states, and we aim to leverage them to develop effective and physics-guided BMS to ensure the safe and reliable operation of battery-powered devices. Similar overviews on other novel sensors and their potential for monitoring and diagnosing battery states will be given in our future studies.

Acknowledgments

The authors acknowledge funding from European Union's Horizon 2020 research and innovation program under grant agreement No 957221. Xia Zeng would also like to thank Simon Feiler, Lukas Gold, and Philip Daubinger from Fraunhofer Institute, Würzburg (Germany) for thoughtful discussions and hands-on training on the ultrasonic experiments.

References

[1] F. Duffner, N. Kronemeyer, J. Tübke, J. Leker, M. Winter, and R. Schmuch, "Post-lithium-ion battery cell production and its compatibility with lithium-ion cell production infrastructure," *Nature Energy*, vol. 6, no. 2, pp. 123–134, 2021.

[2] V. Sulzer, P. Mohtat, A. Aitio, S. Lee, Y. T. Yeh, F. Steinbacher, M. U. Khan, J. W. Lee, J. B. Siegel, A. G. Stefanopoulou *et al.*, "The challenge and opportunity of battery lifetime prediction from field data," *Joule*, 2021.

[3] A. Kwade, W. Haselrieder, R. Leithoff, A. Modlinger, F. Dietrich, and K. Droeder, "Current status and challenges for automotive battery production technologies," *Nature Energy*, vol. 3, no. 4, pp. 290–300, 2018.

[4] C.-Y. Wang, T. Liu, X.-G. Yang, S. Ge, N. V. Stanley, E. S. Rountree, Y. Leng, and B. D. McCarthy, "Fast charging of energy-dense lithium-ion batteries," *Nature*, vol. 611, no. 7936, pp. 485–490, 2022.

[5] M. Herberz, U. J. Hahnel, and T. Brosch, "Counteracting electric vehicle range concern with a scalable behavioural intervention," *Nature Energy*, vol. 7, no. 6, pp. 503–510, 2022.

[6] M. Hao, J. Li, S. Park, S. Moura, and C. Dames, "Efficient thermal management of li-ion batteries with a passive interfacial thermal regulator based on a shape memory alloy," *Nature Energy*, vol. 3, no. 10, pp. 899–906, 2018.

[7] C. Grey and J. Tarascon, "Sustainability and in situ monitoring in battery development," *Nature materials*, vol. 16, no. 1, pp. 45–56, 2017.

[8] X. Hu, C. Zou, C. Zhang, and Y. Li, "Technological developments in batteries: a survey of principal roles, types, and management needs," *IEEE Power and Energy Magazine*, vol. 15, no. 5, pp. 20–31, 2017.

[9] X. Hu, L. Xu, X. Lin, and M. Pecht, "Battery lifetime prognostics," *Joule*, vol. 4, no. 2, pp. 310–346, 2020.

[10] W. Huang, X. Feng, X. Han, W. Zhang, and F. Jiang, "Questions and answers relating to lithium-ion battery safety issues," *Cell Reports Physical Science*, vol. 2, no. 1, 2021.

[11] J. Vetter, P. Novák, M. R. Wagner, C. Veit, K.-C. Möller, J. Besenhard, M. Winter, M. Wohlfahrt-Mehrens, C. Vogler, and A. Hammouche, "Ageing mechanisms in lithium-ion batteries," *Journal of power sources*, vol. 147, no. 1-2, pp. 269–281, 2005.

[12] M. Winter and J. O. Besenhard, "Electrochemical lithiation of tin and tin-based intermetallics and composites," *Electrochimica Acta*, vol. 45, no. 1-2, pp. 31–50, 1999.

[13] C. Pastor-Fernández, T. F. Yu, W. D. Widanage, and J. Marco, "Critical review of non-invasive diagnosis techniques for quantification of degradation modes in lithium-ion batteries," *Renewable and Sustainable Energy Reviews*, vol. 109, pp. 138–159, 2019.

[14] C. R. Birkl, M. R. Roberts, E. McTurk, P. G. Bruce, and D. A. Howey, "Degradation diagnostics for lithium ion cells," *Journal of Power Sources*, vol. 341, pp. 373–386, 2017.

[15] K. Edström, "Battery 2030+ roadmap," 2020.

[16] J. Fraden and J. Fraden, *Handbook of modern sensors: physics, designs, and applications*. Springer, 2004, vol. 3.

[17] G. L. Plett, "Extended kalman filtering for battery management systems of lipb-based hev battery packs: Part 3. state and parameter estimation," *Journal of Power sources*, vol. 134, no. 2, pp. 277–292, 2004.

[18] Z. Wei, J. Zhao, H. He, G. Ding, H. Cui, and L. Liu, "Future smart battery and management: Advanced sensing from external to embedded multi-dimensional measurement," *Journal of Power Sources*, vol. 489, p. 229462, 2021.

[19] L. De Sutter, G. Berckmans, M. Marinaro, M. Wohlfahrt-Mehrens, M. Berecibar, and J. Van Mierlo, "Mechanical behavior of silicon-graphite pouch cells under external compressive load: Implications and opportunities for battery pack design," *Journal of Power Sources*, vol. 451, p. 227774, 2020.

[20] C.-J. Bae, A. Manandhar, P. Kiesel, and A. Raghavan, "Monitoring the strain evolution of lithium-ion battery electrodes using an optical fiber bragg grating sensor," *Energy technology*, vol. 4, no. 7, pp. 851–855, 2016.

[21] A. Hsieh, S. Bhadra, B. Hertzberg, P. Gjeltema, A. Goy, J. W. Fleischer, and D. A. Steingart, "Electrochemical-acoustic time of flight: in operando correlation of physical dynamics with battery charge and health," *Energy & environmental science*, vol. 8, no. 5, pp. 1569–1577, 2015.

[22] G. Davies, K. W. Knehr, B. V. Tassell, T. Hodson, S. Biswas, A. G. Hsieh, and D. A. Steingart, "State of charge and state of health estimation using electrochemical acoustic time of flight analysis," *Journal of The Electrochemical Society*, vol. 164, no. 12, pp. A2746–A2755, 2017.

[23] Y. Wu, Y. Wang, W. K. Yung, and M. Pecht, "Ultrasonic health monitoring of lithium-ion batteries," *Electronics*, vol. 8, no. 7, p. 751, 2019.

[24] D. P. Finegan, J. Zhu, X. Feng, M. Keyser, M. Ulmefors, W. Li, M. Z. Bazant, and S. J. Cooper, "The application of data-driven methods and physics-based learning for improving battery safety," *Joule*, vol. 5, no. 2, pp. 316–329, 2021.

[25] J. Huang, S. T. Boles, and J.-M. Tarascon, "Sensing as the key to battery lifetime and sustainability," *Nature Sustainability*, vol. 5, no. 3, pp. 194–204, 2022.

[26] C. Forgez, D. V. Do, G. Friedrich, M. Morcrette, and C. Delacourt, "Thermal modeling of a cylindrical lifepo4/graphite lithium-ion battery," *Journal of Power Sources*, vol. 195, no. 9, pp. 2961–2968, 2010.

[27] U. S. Kim, C. B. Shin, and C.-S. Kim, "Modeling for the scale-up of a lithium-ion polymer battery," *Journal of Power Sources*, vol. 189, no. 1, pp. 841–846, 2009.

[28] X. Lin, Y. Kim, S. Mohan, J. B. Siegel, and A. G. Stefanopoulou, "Modeling and estimation for advanced battery management," *Annual Review of Control, Robotics, and Autonomous Systems*, vol. 2, pp. 393–426, 2019.

[29] M. Bauer, M. Wachtler, H. Stöwe, J. V. Persson, and M. A. Danzer, "Understanding the dilation and dilation relaxation behavior of graphite-based lithium-ion cells," *Journal of Power Sources*, vol. 317, pp. 93–102, 2016.

[30] B. Rieger, S. Schlueter, S. V. Erhard, J. Schmalz, G. Reinhart, and A. Jossen, "Multi-scale investigation of thickness changes in a commercial pouch type lithium-ion battery," *Journal of Energy Storage*, vol. 6, pp. 213–221, 2016.

[31] R. R. Richardson, P. T. Ireland, and D. A. Howey, "Battery internal temperature estimation by combined impedance and surface temperature measurement," *Journal of Power Sources*, vol. 265, pp. 254–261, 2014.

[32] A. Raghavan, P. Kiesel, L. W. Sommer, J. Schwartz, A. Lochbaum, A. Hegyi, A. Schuh, K. Arakaki, B. Saha, A. Ganguli *et al.*, "Embedded fiber-optic sensing for accurate internal monitoring of cell state in advanced battery management systems part 1: Cell embedding method and performance," *Journal of Power Sources*, vol. 341, pp. 466–473, 2017.

[33] A. Ganguli, B. Saha, A. Raghavan, P. Kiesel, K. Arakaki, A. Schuh, J. Schwartz, A. Hegyi, L. W. Sommer, A. Lochbaum *et al.*, "Embedded fiber-optic sensing for accurate internal monitoring of cell state in advanced battery management systems part 2: Internal cell signals and utility for state estimation," *Journal of Power Sources*, vol. 341, pp. 474–482, 2017.

[34] G. Han, J. Yan, Z. Guo, D. Greenwood, J. Marco, and Y. Yu, "A review on various optical fibre sensing methods for batteries," *Renewable and Sustainable Energy Reviews*, vol. 150, p. 111514, 2021.

[35] Y. D. Su, Y. Preger, H. Burroughs, C. Sun, and P. R. Ohodnicki, "Fiber optic sensing technologies for battery management systems and energy storage applications," *Sensors*, vol. 21, no. 4, p. 1397, 2021.

[36] J. L. Rose, "Ultrasonic waves in solid media," 2000.

[37] J. Achenbach, *Wave propagation in elastic solids*. Elsevier, 2012.

[38] P. Jiao, K.-J. I. Egbe, Y. Xie, A. Matin Nazar, and A. H. Alavi, "Piezoelectric sensing techniques in structural health monitoring: A state-of-the-art review," *Sensors*, vol. 20, no. 13, 2020.

[39] A. Raghavan, "Guided-wave structural health monitoring," Ph.D. dissertation, 2007.

[40] P. Panda and B. Sahoo, "Pzt to lead free piezo ceramics: a review," *Ferroelectrics*, vol. 474, no. 1, pp. 128–143, 2015.

[41] K. W. Knehr, T. Hodson, C. Bommier, G. Davies, A. Kim, and D. A. Steingart, "Understanding full-cell evolution and non-chemical electrode crosstalk of li-ion batteries," *Joule*, vol. 2, no. 6, pp. 1146–1159, 2018.

[42] C. Bommier, W. Chang, J. Li, S. Biswas, G. Davies, J. Nanda, and D. Steingart, "Operando acoustic monitoring of sei formation and long-term cycling in nmc/sigr composite pouch cells," *Journal of The Electrochemical Society*, vol. 167, no. 2, p. 020517, 2020.

[43] P. Ladpli, C. Liu, F. Kopsaftopoulos, and F.-K. Chang, "Estimating lithium-ion battery state of charge and health with ultrasonic waves using an efficient matching pursuit technique," in *2018 IEEE Transportation Electrification Conference and Expo, Asia-Pacific (ITEC Asia-Pacific)*. IEEE, 2018, pp. 1–5.

[44] D. Sauerteig, S. Ivanov, H. Reinshagen, and A. Bund, "Reversible and irreversible dilation of lithium-ion battery electrodes investigated by in-situ dilatometry," *Journal of Power Sources*, vol. 342, pp. 939–946, 2017.

[45] S. Feiler, P. Daubinger, L. Gold, S. Hartmann, and G. A. Giffin, "Interplay between elastic and electrochemical properties during active material transitions and aging of a lithium-ion battery," *Batteries & Supercaps*, p. e202200518, 2023.

[46] L. Gold, T. Bach, W. Virsik, A. Schmitt, J. Müller, T. E. Staab, and G. Sextl, "Probing lithium-ion batteries' state-of-charge using ultrasonic transmission–concept and laboratory testing," *Journal of Power Sources*, vol. 343, pp. 536–544, 2017.

[47] J. C. Jackson, R. Summan, G. I. Dobie, S. M. Whiteley, S. G. Pierce, and G. Hayward, "Time-of-flight measurement techniques for airborne ultrasonic ranging," *IEEE transactions on ultrasonics, ferroelectrics, and frequency control*, vol. 60, no. 2, pp. 343–355, 2013.

Presenter Biography

Xia Zeng received her Master's degree in Vehicle Engineering from Chongqing University, China in 2019. She was a visiting research student with the Department of Electrical Engineering, Chalmers University of Technology, Sweden, between 2017 and 2018. In 2021, she started pursuing a Ph.D. in the Department of Electrical Engineering and Energy Technology (ETEC) at the Vrije Universiteit Brussel, Belgium. Her current research focuses on battery monitoring and states estimation through advanced sensing techniques.